0022-3565/11/3362-468–478$20.00
THE JOURNAL OF PHARMACOLOGY AND EXPERIMENTAL THERAPEUTICS
Vol. 336, No. 2
172817/3657544
Printed in U.S.A.

JPET 336:468–478, 2011

Pharmacological Characterization of KLYP961, a Dual Inhibitor of Inducible and Neuronal Nitric-Oxide Synthases[S]

Kent T. Symons,[1] Phan M. Nguyen, Mark E. Massari,[1] John V. Anzola,[2] Lena M. Staszewski,[3] Li Wang, Nahid Yazdani, Steven Dorow, Jerry Muhammad,[4] Marciano Sablad,[5] Natasha Rozenkrants,[5] Celine Bonefous,[6] Joseph E. Payne,[7] Peter J. Rix,[6] Andrew K. Shiau,[2] Stewart A. Noble, Nicholas D. Smith,[6] Christian A. Hassig,[8] Yan Zhang,[5] and Tadimeti S. Rao[5]

Departments of Biology (K.T.S., P.M.N., M.E.M., J.V.A., L.M.S., A.K.S., C.A.H.), Drug Metabolism and Pharmacokinetics (L.W., P.J.R.), Pharmaceutical Sciences (N.Y., S.D., J.M.), Chemistry (C.B., J.E.P., S.A.N., N.D.S.), and Pharmacology (M.S., N.R., Y.Z., T.S.R.), Kalypsys Inc., San Diego, California

Received July 12, 2010; accepted October 21, 2010

ABSTRACT

Nitric oxide (NO) derived from neuronal nitric-oxide synthase (nNOS) and inducible nitric-oxide synthase (iNOS) plays a key role in various pain and inflammatory states. KLYP961 (4-((2-cyclobutyl-1*H*-imidazo[4,5-b]pyrazin-1-yl)methyl)-7,8-difluoroquinolin-2(1*H*)-one) inhibits the dimerization, and hence the enzymatic activity of human, primate, and murine iNOS and nNOS (IC_{50} values 50–400 nM), with marked selectivity against endothelial nitric-oxide synthase (IC_{50} >15,000 nM). It has ideal drug like-properties, including excellent rodent and primate pharmacokinetics coupled with a minimal off-target activity profile. In mice, KLYP961 attenuated endotoxin-evoked increases in plasma nitrates, a surrogate marker of iNOS activity in vivo, in a sustained manner (ED_{50} 1 mg/kg p.o.). KLYP961 attenuated pain behaviors in a mouse formalin model (ED_{50} 13 mg/kg p.o.), cold allodynia in the chronic constriction injury model (ED_{50} 25 mg/kg p.o.), or tactile allodynia in the spinal nerve ligation model (ED_{50} 30 mg/kg p.o.) with similar efficacy, but superior potency relative to gabapentin, pregabalin, or duloxetine. Unlike morphine, the antiallodynic activity of KLYP961 did not diminish upon repeated dosing. KLYP961 also attenuated carrageenin-induced edema and inflammatory hyperalgesia and writhing response elicited by phenylbenzoquinone with efficacy and potency similar to those of celecoxib. In contrast to gabapentin, KLYP961 did not impair motor coordination at doses as high as 1000 mg/kg p.o. KLYP961 also attenuated capsaicin-induced thermal allodynia in rhesus primates in a dose-related manner with a minimal effective dose (≤10 mg/kg p.o.) and a greater potency than gabapentin. In summary, KLYP961 represents an ideal tool with which to probe the physiological role of NO derived from iNOS and nNOS in human pain and inflammatory states.

Introduction

Three mammalian nitric-oxide synthases (NOSs), neuronal NOS (nNOS; NOS-1), inducible NOS (iNOS; NOS-2), and endothelial NOS (eNOS; NOS-3), are involved in the generation of NO, a diffusible second-messenger molecule with diverse pharmacological actions. All three isoforms are active only as homodimers and use L-arginine as the sole common substrate. The overproduction of NO has been implicated in multiple human pathologies such as pain, inflammation, arthritis, asthma, chronic obstructive pulmonary disease, migraine, and neurodegenerative disorders (Vallance and Leiper, 2002). Of particular relevance to pain and inflamma-

[1]Current affiliation: Dart Neuroscience, San Diego, California.
[2]Current affiliation: Ludwig Institute for Cancer Research, La Jolla, California.
[3]Current affiliation: Traversa Therapeutics, San Diego, California.
[4]Current affiliation: Inhibitex Inc., Alpharetta, Georgia.
[5]Current affiliation: Johnson and Johnson Pharmaceutical Research and Development, San Diego, California.
[6]Current affiliation: Aragon Pharmaceuticals, San Diego, California.
[7]Current affiliation: Nitto Denko Technical Corporation, Carlsbad, California.
[8]Current affiliation: Conrad Prebys Chemical Genomics Center, Sanford Burnham Research Center, San Diego, California.
Article, publication date, and citation information can be found at http://jpet.aspetjournals.org.
doi:10.1124/jpet.110.172817.
[S] The online version of this article (available at http://jpet.aspetjournals.org) contains supplemental material.

ABBREVIATIONS: NOS, nitric-oxide synthase; iNOS, inducible NOS; eNOS, endothelial NOS; nNOS, neuronal NOS; CCI, chronic constrictive nerve injury; PBQ, phenylbenzoquinone; BBS-4, (*R*)-1-(2-(1*H*-imidazol-1-yl)-6-methylpyrimidin-4-yl)-*N*-(2-(benzo[*d*][1,3]dioxol-5-yl)ethyl)pyrrolidine-2-carboxamide; HEK, human embryonic kidney; SEITU, 2-ethyl-2-thiopseudourea hydrobromide; LPS, lipopolysaccharide; MK-801, (+)-5-methyl-10,11-dihydro-5*H*-dibenzo[a,d]cyclohepten-5,10-imine maleate; ANOVA, analysis of variance; AUC, areas under the curve; DMSO, dimethyl sulfoxide; KLYP956, *N*-(3-chlorophenyl)-*N*-((8-fluoro-2-oxo-1,2-dihydroquinolin-4-yl)methyl)-4-methylthiazole-5-carboxamide; HA, hemagglutinin; CI, confidence interval; KLYP961 (4-((2-cyclobutyl-1*H*-imidazo[4,5-b]pyrazin-1-yl)methyl)-7,8-difluoroquinolin-2(1*H*)-one; GW274150, ([2-[(1-iminoethyl) amino]ethyl]-L-homocysteine).

tion, 1) NO is involved in the transmission and modulation of nociceptive information at peripheral, spinal, and supraspinal levels (Yamamoto et al., 1993; Goettl and Larson, 1996; Wu et al., 2001), 2) NO contributes to the development and maintenance of central sensitization (Haley et al., 1992; Malmberg and Yaksh, 1993; Meller and Gebhart, 1993; Wu et al., 2001) and peripheral neuropathic pain (Levy and Zochodne, 1998; Levy et al., 1999), 3) NO is a pronociceptive mediator that synergizes with hyperalgesic prostaglandins in nociceptor sensitization (Aley et al., 1998), and importantly, 4) NO-donating compounds induce hyperalgesia and migraine in humans and hyperalgesia in nonhuman primates and rodents (Holthusen and Arndt, 1994; Kawabata et al., 1994; Aley et al., 1998; Lin et al., 1999). Antinociceptive activity of structurally diverse iNOS-selective inhibitors, as well as nonselective NOS inhibitors (Tao et al., 2003; De Alba et al., 2006; LaBuda et al., 2006; Tang et al., 2007), provides further rationale for the pursuit of NOS inhibitors as therapeutics for pain and inflammation. Currently, one iNOS active-site inhibitor, GW274150, ([2-[(1-iminoethyl) amino]ethyl]-L-homocysteine) is in clinical trials.

Of the three isoforms, iNOS and nNOS are the most intimately associated with inflammation and pain. Stoichiometrically, iNOS generates the highest amount of NO, and an important role for iNOS in the pathophysiology of inflammatory and neuropathic pain is supported by its expression in glia and perineural Schwann cells after peripheral nerve injury and at sites associated with axonal degeneration (Levy and Zochodne, 1998; Levy et al., 1999) and by a low, constitutive expression in the spinal cord of naive animals with rapid up-regulation upon injury (Tang et al., 2007). Chronic pain often is associated with persistent activation of *N*-methyl-D-aspartate receptor and downstream nNOS-derived production of NO, which in turn, augments further glutamate release, thus setting a stage for multisynaptic nociceptive processing in the spinal cord. NO derived from eNOS is critical for the maintenance of blood pressure, and its inhibition leads to hypertension. Therefore, NOS inhibitor-based therapeutics must selectively inhibit iNOS and/or nNOS isoforms, while sparing eNOS.

Drug discovery efforts to identify inhibitors of iNOS and nNOS have focused largely on mimicry of arginine, the common substrate for all three isoforms, and the efficacy of selective or nonselective inhibitors of iNOS that act via such mechanisms has been extensively examined in preclinical models of pain and inflammation (see above). However, biosynthesis of NO via NOS enzymes is a highly regulated process involving dimerization of enzymes, substrate, and cofactor dependence (e.g., tetrahydrobiopterin and calmodulin), the requirement of calcium for eNOS and nNOS, but not for iNOS, and regulation of expression of iNOS by inflammatory cytokines. Another level of post-translational regulation occurs via turnover of the dimer. Although all NOS isoforms are active only as functional homodimers, the three isoforms seem to differ in the cellular turnover rates of their respective dimers. For example, in primary human bronchial epithelial cells, the cellular half-life for iNOS dimers was reported to be ~1.6 h, which contrasts with reported values of 28 h for eNOS and 20 h for nNOS (Kolodziejski et al., 2004). The feasibility of inhibition or destabilization of the iNOS dimerization process, a protein-protein interaction process, by small-molecule ligands has been successfully demonstrated (Davey et al., 2007; Symons et al., 2009). Rapid cellular turnover of the iNOS dimer suggests the possibility of achieving superior isoform selectivity by targeting the dimerization process. In vivo, the potential also exists for this novel mechanism of inhibition of NOS to engender a differential profile relative to substrate competitive inhibitors. A cell-based, high-throughput screen of recombinant human iNOS transiently expressed in human embryonic kidney (HEK) cells led to the identification of *N*-(3-chlorophenyl)-*N*-((8-fluoro-2-oxo-1,2-dihydroquinolin-4-yl)methyl)-4-methylthiazole-5-carboxamide (KLYP956), a nonimidazolylpyrimidine, quinolone inhibitor of iNOS that acts via inhibition or destabilization of dimerization (Symons et al., 2009). Optimization of KLYP956 for desirable drug-like properties culminated in the identification of KLYP961 (Bonefous et al., 2009; Payne et al., 2010) (Fig. 1). This article describes its pharmacological profile.

Materials and Methods

Materials

KLYP961 HCl salt, KLYP322, KLYP775, and celecoxib were synthesized at Kalypsys Inc (Bonefous et al., 2009; Payne et al., 2010). AZ102222C (LaBuda et al., 2006), a substrate competitive inhibitor, and (*R*)-1-(2-(1*H*-imidazol-1-yl)-6-methylpyrimidin-4-

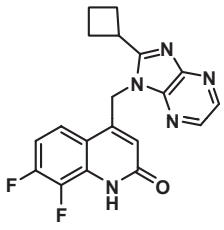

KLYP961

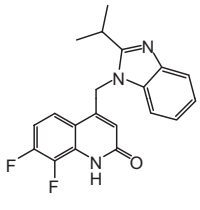

KLYP 322

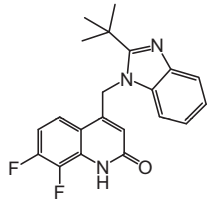

KLYP 775

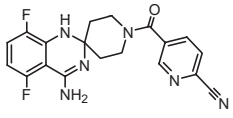

AZ1022222c

Fig. 1. Chemical structures of KLYP961 (top left), KLYP322 (top center), KLYP775 (top right), and AZ1022222C (bottom).

yl)-*N*-(2-(benzo[*d*][1,3]dioxol-5-yl)ethyl)pyrrolidine-2-carboxamide (BBS-4) (Davey et al., 2007), a reference N-substituted imidazole-based iNOS dimerization inhibitor, were synthesized at Kalypsys per published methods (Davey et al., 2007). The sources of other pharmacological agents were as follows: gabapentin (Sigma-Aldrich, St. Louis, MO), capsaicin (Sigma-Aldrich), pregabalin and duloxetine HCl (both from QV Chemicals, St. Louis, MO), (+)-5-methyl-10,11-dihydro-5*H*-dibenzo[a,d]cyclohepten-5,10-imine maleate (MK-801) (Sigma-Aldrich), and phenylbenzoquinone (PBQ) (Acros Organics, Fairlawn, NJ). All other laboratory reagents were of the highest quality commercially available.

In Vitro Studies

Molecular Cloning. Human and murine iNOS, nNOS, and eNOS were cloned as described previously (Symons et al., 2009).

Cell Culture. RAW 264.7 (murine macrophage) and HEK293 cells (American Type Culture Collection, Manassas, VA) were cultured in Dulbecco's modified Eagle's medium containing 10% fetal bovine serum, 100 U/ml penicillin, and 100 μg/ml streptomycin. RAW 264.7 cells were stimulated in media with lipopolysaccharide (LPS) (1 μg/ml) (Sigma-Aldrich) and murine interferon-γ (100 U/ml) (Roche Diagnostics, Indianapolis, IN).

NOS Assay in Transiently Transfected HEK293 Cells. HEK293 cells were transiently transfected with a cytomegalovirus-driven plasmid expressing a specific NOS isozyme. For iNOS, 10 μg of human, murine, rat, or rhesus iNOS expression plasmids and 30 μl of Fugene 6 were used. For eNOS, 15 μg of human, murine, or cynomolgus eNOS expression plasmids and 45 μl of Fugene 6 were used. For nNOS, 10 μg of human, murine, rat, or cynomolgus nNOS expression plasmids and 30 μl of Fugene 6 were used. The effect of test compounds on NOS activity was assessed by measurement of accumulated nitrates in the tissue culture media using the diaminonaphthalene assay as described previously (Symons et al., 2009).

Cytochrome P450 Inhibition Assay. The potential for KLYP961 to inhibit human cytochrome P450 enzymes was assessed in pooled human liver microsomes using isoform-specific substrates as summarized in Supplemental Methods S1.

Gel-Based Dimer Assay (Low-Temperature SDS-Polyacrylamide Gel Electrophoresis) for iNOS and nNOS. The impact of KLYP961 or other NOS inhibitors on murine iNOS dimer stability was assessed in the murine macrophage cell line (RAW 264.7) as described previously (Symons et al., 2009). Additional details are provided in Supplemental Methods S2.

In Vivo Studies

Rodents. Male BALB/c and C57BL6/J mice (iNOS and nNOS knockout mice and appropriate age-/sex-matched wild-type controls; weighing 19–25 g) were obtained from Charles River Breeding Laboratories (Portage, MI) and The Jackson Laboratory (Bar Harbor, ME), respectively. All animals were acclimated to the Kalypsys vivarium for a minimum of 5 days before use in the experiments that were conducted per institutionally approved animal care and use protocols.

Primates. Male Rhesus monkeys (*Macaca mulatta*; 3–5 kg) were used in pharmacology studies, and pharmacokinetic studies used both male rhesus and cynomolgus nonhuman primates. All primate studies were conducted under a collaborative agreement between Kalypsys and Yunnan Laboratory Primate Laboratory Inc. (Kunming City, China) per guidelines for primate health/welfare and use in animal experimentation implemented by relevant regulatory authorities. Additional studies were conducted at the Biological Resources Laboratory of the University of Illinois (Chicago, IL) under a collaborative research agreement between Kalypsys and CorDynamics (Chicago, IL), and the study was governed by the U.S. Drug Administration Animal Welfare Act and the Institute of Laboratory Animal Research *Guide for the Care and Use of Laboratory Animals*.

Drug Substance, Dose Formulations, and Pharmacokinetic Studies. A HCl salt form of KLYP961 was used in the studies described herein, and doses refer to its neutral form. Details of oral and intravenous formulations and methodology for pharmacokinetic profiling are summarized in Supplemental Methods S3.

Pharmacology Studies. The effects of KLYP961 were examined in the mouse LPS model for the inhibition of iNOS enzyme activity in vivo. Effects on pain processing were determined in a mouse formalin model, the chronic constrictive nerve injury (CCI) model, the Chung model (Kim and Chung, 1992), and a primate model of capsaicin-induced thermal hyperalgesia. The effects on inflammation were assessed in carrageenan-induced paw edema and hyperalgesia and in PBQ-induced peritoneal writhing models. Detailed methods for these models are summarized in Supplemental Methods S4.

Mouse LPS Test. Injection of LPS activates a cascade of inflammatory pathways, leading to production of cytokines such as tumor necrosis factor α, interleukin-1, and interleukin-6, and induces enzymes such as iNOS. The latter is reflected in time-dependent increases in plasma nitrates.

Mouse Pain Studies

Formalin Assay. Three experiments were conducted in the mouse formalin model. The first experiment defined the potency of gabapentin and pregabalin, two clinically used benchmarks. The second experiment defined the potency of KLYP961 (3, 10, 30, and 100 mg/kg). In both cases, all treatments were given orally 15 min before intraplantar injection of formalin. The third experiment defined the duration of action of KLYP961 (30 mg/kg) administered 0.25, 4, and 6 h in advance of the formalin injection.

Nerve Injury Models. Initial experiments in the Bennett model (Bennett and Xie, 1988) explored mechanical allodynia and cold allodynia as the indices of nerve injury-evoked neuropathic pain state. As the acetone-induced cold allodynia was found to be more robust and consistent response than the mechanical allodynia, all efficacy studies used cold allodynia as the endpoint. In the Chung model (Kim and Chung, 1992), nerve ligation-induced tactile allodynia was assessed as the endpoint. In both models, dose-related effects of KLYP961were examined. In addition, studies were conducted to examine whether antinociceptive effects of KLYP961 in nerve injury tolerate upon repeated dosing. In these assays, the effects of KLYP961 were compared with selected reference compounds such as gabapentin, pregabalin, and duloxetine.

Carrageenin-Induced Paw Inflammation and Phenylbenzoquinone-Induced Peritoneal Writhing Assays. Anti-inflammatory activity of KLYP961 (dose range: 10–300 mg/kg p.o.) was assessed in two pharmacological models: 1) λ-carrageenan-induced paw edema and thermal hyperalgesia and 2) PBQ-induced peritoneal writhing. Celecoxib (dose range 3–300 mg/kg p.o.) was used as the reference compound.

Primate Efficacy Studies

Capsaicin-Induced Thermal Hyperalgesia in Rhesus Nonhuman Primates. The effects of KLYP961, gabapentin, and MK-801 on capsaicin-induced thermal hyperalgesia were examined in rhesus nonhuman primates based on the methodology developed by Butelman et al. (2003).

Effects of Dizocilipine (MK-801). Efficacy of MK-801 (0.06 mg/kg s.c.) was evaluated on established thermal allodynia. Fifteen minutes after the removal of capsaicin thermal allodynia was rated. Animals were randomized to receive either vehicle ($n = 2$ animals) or MK-801 (1 ml/kg, saline solution; $n = 4$ animals). The treatment-related effects were monitored over 6 h.

Effects of Gabapentin. Efficacy of gabapentin was evaluated in prophylactic mode of administration. In this paradigm, animals were given an oral dose of gabapentin (dissolved in distilled water; 60 mg/kg/day; $n = 4$ animals) or vehicle (distilled water; $n = 2$ animals) for 3 consecutive days, via nasogastric tube. Baseline thermal with-

drawal latencies were recorded on days 2 and 3, and the average latency was used in defining treatment effect. On day 3, 45 min after the oral dose of either gabapentin or water all animals received topical application of capsaicin, and changes in withdrawal latencies were determined. In a separate study, efficacy of a single dose of gabapentin (60 mg/kg p.o.) was also evaluated. For this study, animals received either gabapentin ($n = 4$) or water ($n = 3$) 45 min before topical application of capsaicin.

Effects of KLYP961. Efficacy of KLYP961 was examined under two experimental conditions. In the first instance, four different doses (3, 10, 30, and 100 mg/kg; suspension) were orally administered via a nasogastric tube. The control group of animals received appropriate vehicle (Supplemental Section S3). The treatments were given 45 min before the capsaicin patch was applied. The entire experiment was completed in four cycles with two animals in the control group and four animals in each of the KLYP961 treatment groups, with at least 7days of washout between cycles. In each cycle, animals were randomized and rotated between control and KLYP961 treatment groups. Pooled data from the control group of animals in the entire experiment ($n = 8$) were used to determine relative effects of KLYP961 on allodynia.

In the second experiment, the efficacy of KLYP961 was evaluated on established thermal allodynia at a dose of 30 mg/kg given orally. On the study day, the capsaicin patch was applied for 15 min and then removed (time 0). Thermal allodynia was assessed 45 min after patch removal. Fifteen minutes later, i.e., 60 min after capsaicin removal, animals received either vehicle (5 ml/kg; $n = 4$ animals) or KLYP961 (30 mg/kg as a suspension; 5 ml/kg; $n = 7$ animals), and allodynia was measured after 1.5, 2, 3, and 4 h (all times relative to time 0, i.e., capsaicin patch removal).

Side Effect Profile Studies. Potential side effects of KLYP961 on gastrointestinal transit and motor coordination were explored in mouse models, whereas the impact on cardiovascular function was assessed in telemetered cynomolgus primates. The relevant methods are summarized in Supplemental Methods S5.

Gastrointestinal Transit Test in Mice. The impact of repeated administration of KLYP961 on gastric motility was assessed using the charcoal meal transit assay. KLYP961 was dosed at 15, 50, and 150 mg/kg b.i.d. (total daily doses of 30, 100 and 300 mg/kg p.o.) for 6 days followed by one additional dose on day 7. Morphine sulfate was used as the reference compound and was dosed once (5.5 mg/kg s.c.).

Motor Coordination: Mouse Rotorod. Effects of KLYP961 on motor coordination were assessed in the rotarod assay (Dunham and Miya, 1957).

Primate Safety Studies: Cardiovascular Studies in Telemetered Cynomolgus Primates

NO derived via eNOS is essential to maintain vascular tone, and its inhibition leads to dose-limiting increases in blood pressure. Because eNOS enzyme has slow turnover, repeat-dose, dose-escalation studies were conducted in telemetered cynomolgus nonhuman primates. The dose levels were 0 (vehicle), 23, 72, and 96 mg/kg p.o. per day of KLYP961 (4 days at each level). The systemic hemodynamic variables of mean arterial pressure, systolic arterial pressure, diastolic arterial pressure, and heart rate and several electrocardiographic parameters such as PR interval, QRS duration, QT/QTc interval, and arrhythmogenesis were examined continuously throughout the doing phase of this study.

Data Analyses

Data represent mean ± S.D. or S.E. and were analyzed by appropriate statistical tests [one-way or two-way analysis of variance (ANOVA)] followed by post hoc tests (Dunnett's/Bonferroni's or t test). Statistical significance relative to either control or other treatments was inferred at $p \leq 0.05$. The number of replicates is indicated, and the time points for sampling that were used in areas under the curve (AUC) estimates (Prism; GraphPad Software Inc., San Diego, CA) are identified in relevant figure legends.

Results

NOS Selectivity Profile

The inhibitory activity of KLYP961 against iNOS and nNOS and selectivity against eNOS in various species was examined using nitrite measurements as surrogate for NOS activity. The results are summarized Table 1.

KLYP961 inhibits iNOS and nNOS with superior selectivity against eNOS. The iNOS to eNOS selectivity ratios in human, primate, and mouse enzymes were 184, 290, and 37, respectively. The iNOS-to-eNOS selectivity ratio in rat enzymes has not been determined. The iNOS-to-nNOS selectivity ratios in human, primate, rat, and mouse enzymes were 3, 1.4, 0.04, and 0.07, respectively. KLYP961 exhibits species-dependent differences in iNOS/nNOS selectivity and potency; KLYP961 is a more potent murine nNOS versus iNOS inhibitor, whereas the selectivity is reversed in humans or in primates.

Mechanism of NOS Inhibition: Inhibition of Dimerization

The inhibitory potencies for KLYP961 in cell-based assays were strongly influenced by the timing of its addition relative to NOS expression, i.e., its inclusion with cell lines during expression of NOS provides robust inhibition of NOS enzyme activity, whereas incubation after NOS expression results in significantly reduced inhibition (e.g., 100% inhibition versus 15% inhibition at 100 μM, respectively). This inhibition signature is similar to that seen for the pyrimidine imidazole dimerization inhibitors and contrasts with substrate competitive inhibitors that show little change in potency or efficacy under these conditions (Symons et al., 2009).

Low-temperature SDS-polyacrylamide gel electrophoresis provides a more direct means of investigating compound effects on the quaternary structure of NOS enzymes. Treatment with KLYP961 or the pyrimidine imidazole BBS-4, but not 2-ethyl-2-thiopseudourea hydrobromide (SEITU) (substrate competitive inhibitor), during the induction of iNOS in the murine RAW264.7 cells resulted in the appearance of

TABLE 1
Inhibitory activity of KLYP961 on NOS isoforms
Numbers of experiments run in triplicate/quadruplicate are shown in parentheses.

Human NOS			Nonhuman Primate NOS			Rat NOS		Mouse NOS		
iNOS ($n = 28$)	eNOS ($n = 20$)	nNOS ($n = 20$)	iNOS[a] ($n = 5$)	eNOS[b] ($n = 2$)	nNOS[a] ($n = 3$)	iNOS ($n = 4$)	nNOS ($n = 2$)	iNOS ($n = 15$)	eNOS ($n = 3$)	nNOS ($n = 3$)
IC_{50}, μM										
0.09 ± 0.04	16.6 ± 6.0	0.30 ± 0.14	0.05 ± 0.02	14.5 ± 4.0	0.07 ± 0.06	1.7 ± 0.66	0.06 ± 0.02	0.43 ± 0.36	16.0 ± 9.9	0.03 ± 0.02

[a] Rhesus.
[b] Cynomolgus.

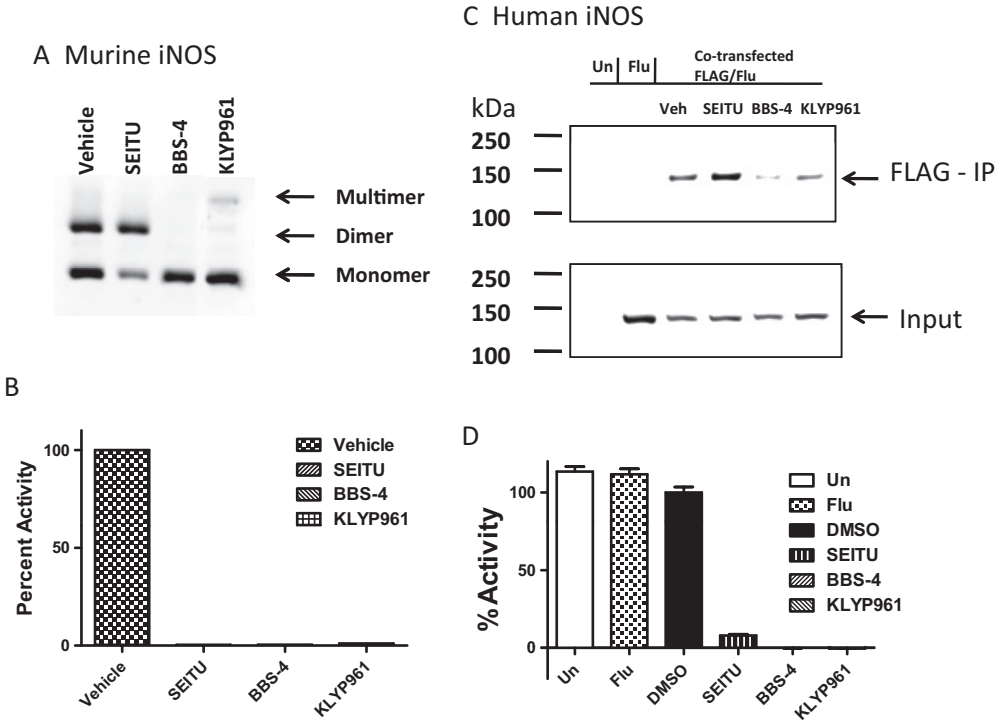

Fig. 2. A and C, KLYP961 affects murine (A) or human (C) iNOS dimer stability. B and D, enzyme activity was measured by quantitation of nitrates in the medium. Cotransfected FLAG/Flu samples were treated with either 0.5% DMSO (Veh), 50 μM SEITU, 0.5 μM BBS-4, or 10 μM KLYP961. C, Western blot analysis with a Flu-specific monoclonal antibody reveals dimeric human iNOS after FLAG immunoprecipitation. The crude lysate input is included as a control for the amount of Flu-tagged iNOS that was present before immunoprecipitation (indicated in the bottom Western blot). Untagged and Flu-tagged alone were treated with 0.5% DMSO and are included as controls. Molecular mass is indicated in kDa. The expected molecular mass of human iNOS is ~130 kDa.

higher-order multimers in the KLYP961-treated samples accompanied by a reduction in dimeric enzyme (Fig. 2A). These findings parallel results obtained with its parent molecule, KLYP956 (Symons et al., 2009). As expected, all three inhibitors block NO production (Fig. 2B). KLYP961 and BBS-4 also destabilize human iNOS protein-protein interactions under more native conditions. The experiment involved transient cotransfection of HEK293 cells with FLAG-tagged and HA-tagged human iNOS enzymes. Lysates prepared from cotransfected cells allows coimmunoprecipitation of the HA-tagged enzyme using anti-FLAG antibodies provided the enzyme is capable of dimerization (Fig. 2A). Neither HA-tagged nor untagged native human iNOS coimmunoprecipitated with anti-FLAG antibodies in the absence of coexpressed FLAG-tagged human iNOS (Fig. 2C). Whereas SEITU increases the amount of coimmunoprecipitated HA-iNOS, both KLYP961 and BBS-4 have substantially reduced levels of anti-HA immunoreactivity, consistent with a reduction in dimeric human iNOS. Enzymatic activity from cell culture supernatants treated with SEITU (50 μM), BBS-4 (0.5 μM), and KLYP961 (0.5 μM) all were reduced by >95%, indicating that residual human iNOS-tagged heterodimer/multimers were inactive (Fig. 2D). Collectively, these data indicate that KLYP961 interferes with iNOS dimer formation and/or destabilizes a dimmer, leading to preferential accumulation of functionally inactive iNOS.

Off-Target Activity Profile

The selectivity profile of KLYP961 was examined by determining its interactions at a test concentration of 10 μM with a panel of 50 targets comprised of G protein-coupled receptors, ion channels, and transporters of biogenic amines and enzymes such as monoamine oxidases A and B and cyclooxygenases 1 and 2 (CEREP Screen). Under these conditions, KLYP961 did not show any measurable interaction at any of the targets examined. These results summarized in Supplemental Table S1 indicate that KLYP961 is remarkably selective. In addition, in the concentration range of 10 to 30 μM KLYP 961 was devoid of agonist or antagonist activity at the vanilloid receptor.

CYP Inhibition and Interaction with Pregnane X Receptor. KLYP961 did not exhibit any appreciable inhibitory activity against the six human isoforms examined, CYP1A2, CYP2C8, CYP2C9, CYP2C19, CYP2D6, or CYP3A4. The estimated IC_{50} value for all targets exceeded 30 μM. Furthermore, KLYP96, at concentrations as high as 30 μM, did not bind to human pregnane X receptor and constitutive androstane receptor in a biochemical assay (data not shown).

Microsomal Stability

KLYP961 showed species-dependent in vitro microsomal stability. The half-lives (minutes, mean ± S.D., $n = 3$) were 345 ± 3 (mouse), 151 ± 16 (rat), 63 ± 13 (dog), 160 ± 56 (cynomolgus monkey), and 277 ± 77 (human), respectively.

Plasma Protein Binding

KLYP961 showed species-dependent plasma protein binding differences. The binding was moderate: 84.4% (mouse), 78% (rat), 37.8% (cynomolgus monkey), and 75.3% (human).

Pharmacokinetic Parameters in Mice and Rhesus Nonhuman Primates

Mice and rhesus nonhuman primates were used as preclinical species to define antinociceptive effects of KLYP961. As such, pharmacokinetic profiles of KLYP961 after single-dose administration were evaluated in these two species under fasting conditions. The results summarized in Supplemental Table S2 and Supplemental Fig. S1, A and B indicate that KLYP961 is orally bioavailable, with approximately 60% oral bioavailability in both species. KLYP961 exhibits low systemic clearance in both mice and nonhuman primates, with systemic clearance generally less than 20% of hepatic blood

flow in both species. KLYP961 exhibits substantially higher volume of distribution in primates (calculated V_{ss} ~4 L/kg) versus mice (calculated V_{ss} ~0.4 L/kg), and it is anticipated that relative differences in the plasma-free fractions in these two species (62 versus 16% in cynomolgus monkey and mouse plasma, respectively). KLYP961 has a robust pharmacokinetic profile in all preclinical species examined. Although the oral bioavailability was fairly similar, KLYP961 exhibited a longer half-life and larger volume of distribution in primates versus mice. The pharmacokinetic profile of KLYP961 in rats was fairly similar to that in mice (data not shown).

Based on brain-to-plasma level ratio of KLYP961 in mice, the brain penetration was estimated to be in the range of 1 to 2% (data not shown). Using a more refined technique of intravenous infusion of KLYP961 to achieve steady-state levels and microdialysis of hippocampal parenchyma, brain penetration in rats was determined to be 1% (Supplemental Results S6.1; Supplemental Fig. S1C) These results are also consistent with a lower volume of distribution and smaller plasma-free fraction in rodents. The higher volume of distribution and larger plasma-free fraction in primates suggests the possibility that KLYP961 may be more brain-penetrant in this species.

Mouse Pharmacology Studies: LPS Assay

Orally administered KLYP961 attenuated LPS-induced increases in plasma nitrates in a dose-dependent manner with an ED_{50} value of 0.98 mg/kg (Supplemental Results S6.2; Supplemental Fig. S2A). KLYP961 (30 mg/kg p.o.) inhibited the LPS plasma nitrate response by ≥50% for up to 12 h. At doses as high as 100 mg/kg, KLYP961 did not affect LPS-induced inflammatory cytokine production (Supplemental Fig. S2C).

Formalin Model

Orally administered KLYP961 attenuated formalin-induced nocifensive behaviors in a dose-related manner (Fig. 3, A and B). KLYP961 was more potent than gabapentin or pregabalin at attenuating both phases of nocifensive behaviors. The ED_{50} values (mg/kg p.o.) for inhibition of phase I behaviors by KLYP961, gabapentin, and pregabalin, respectively were 28 [95% confidence intervals (CI): 19–43], 142 (CI: 124–162), and 72 mg/kg (CI: 63–82), respectively. The corresponding ED_{50} values (mg/kg p.o.) for inhibition of phase II behaviors were 12.6 (CI: 9.7–16), 116 (CI: 105–128), and 72 (CI: 63–83), respectively.

The inhibitory effects of KLYP961 on formalin-induced pain behaviors showed time dependence (Fig. 3C); a 30 mg/kg dose significantly inhibited phase II behaviors for up to 4 h, whereas inhibition of phase I behaviors was more transient with only the 15-min pretreatment being effective (two-way ANOVA: phases I and II, $F_{1,26} = 8.8$, $p < 0.0001$; time: $F_{3,26} = 72$, $p < 0.0001$; interaction: $F_{3,26} = 12$, $p < 0.0001$).

With a view toward understanding the causal relationship between NOS inhibition and efficacy of KLYP961in the formalin model, two approaches were used. The first used the chemical approach, and the second used a genetic approach. Two structurally related analogs, KLYP322 and KLYP775

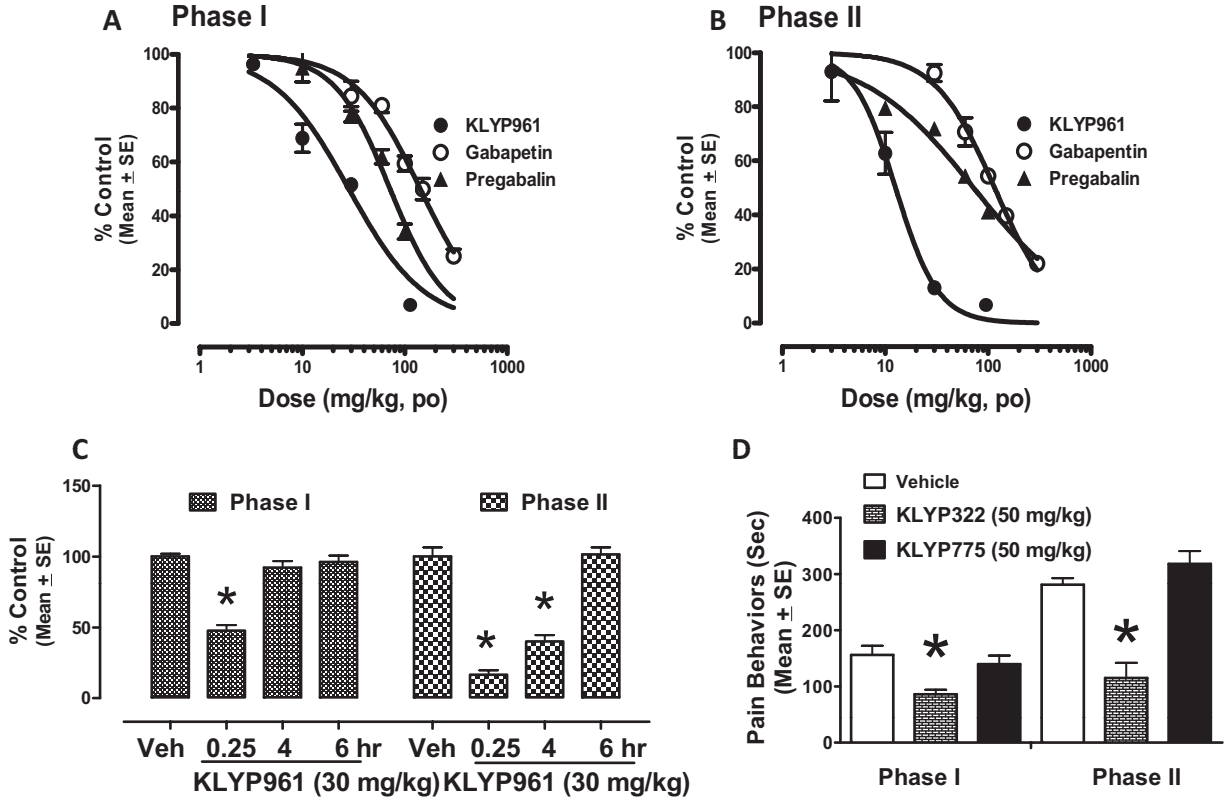

Fig. 3. A and B, KLYP961, gabapentin, and pregabalin dose-dependently attenuate formalin-induced pain behaviors [phase I (A) and phase II (B)]. C, KLYP961 (30 mg/kg p.o.) attenuates formalin-induced phase II behaviors for up to 4 h with a transient effect on phase I. D, inhibitory potency of KLYP322 (IC_{50} 3600 nM, murine iNOS; IC_{50} 160 nM, murine nNOS) and KLYP775 (IC_{50} values of >10,000 nM for both iNOS and nNOS) tracks well with inhibition of pain behaviors. Both compounds were dosed orally 30 min in advance of formalin. Data represent phase II behavior and mean ± S.E. (n = 5–6 all groups; except KLYP961, 100 mg/kg, n = 3). *, $p < 0.05$ versus vehicle (Veh).

(Fig. 1), differing only in their NOS inhibitory profiles, were evaluated in the formalin assay. The IC_{50} values to inhibit murine nNOS and iNOS for KLYP322 were 160 and 3600 nM, respectively. The corresponding values for KLYP775 were >10,000 and >10,000 nM, respectively. At an oral dose of 50 mg/kg that resulted in plasma levels in excess of 20 μM at between 0.5 and 1 h after dose, KLYP322, but not KLYP775, attenuated both phases of formalin-induced pain behaviors ($p < 0.05$; Fig. 3D).

In the second instance, effects of KLYP961 in the formalin assay were compared in iNOS or nNOS knockout mice on C57BL6/J background relative to its profile in appropriate age- and gender-matched C57BL6/J wild-type mice (data not shown). The degree of inhibition of phase II behaviors in both iNOS and nNOS knockout animals was approximately 50% of that seen in C57BL6/J wild-type control mice, suggesting that inhibition of both isoforms contributes to the attenuation of formalin response by KLYP961 (data not shown).

Neuropathic Pain Models in Mice

Chronic constrictive injury of sciatic nerve induces neuropathic pain state, and acetone-induced cold allodynia was used as the endpoint. In time-course experiments, KLYP961 (30 mg/kg p.o.), gabapentin (300 mg/kg p.o.), duloxetine (100 mg/kg p.o.), pregabalin (100 mg/kg p.o.), and morphine sulfate (3 mg/kg s.c.) attenuated cold allodynia with a robust reduction in allodynia seen at 60 to 90 min after dose (data not shown). Therefore, dose-response curves for KLYP961, gabapentin, and duloxetine were generated with allodynia measurements conducted 60 min after dose, whereas a 90-min time point after dose was selected for pregabalin. KLYP961 and benchmark compounds, gabapentin, pregabalin, and duloxetine, attenuated cold allodynia in a dose-related manner (Fig. 4) with similar magnitudes of efficacy. KLYP961 was more potent than benchmarks: ED_{50} values in mg/kg (with confidence intervals) for KLYP961, gabapentin, pregabalin, and duloxetine were 25 (CI:15–38), 254 (CI:117–519), 72 (CI:44–118), and 53 (CI:28–106), respectively.

Efficacy of KLYP961 was also assessed in the Chung model of neuropathic pain induced by spinal nerve ligation (Kim and Chung, 1992). The experimental positive control, gabapentin, attenuated tactile allodynia at the highest dose of 300 mg/kg p.o. (Fig. 5A; dose, $F_{2,48} = 13.9$, $p < 0.0001$; time, $F_{3,48} = 18$, $p < 0.001$; interaction, $F_{6,48} = 14.1$, $p < 0.05$). KLYP961 attenuated tactile allodynia at 30 and 100 mg/kg doses with a peak effect at 30 min (Fig. 5B; dose, $F_{3,104} = 16.3$, $p < 0.0001$; time, $F_{3,104} = 14$, $p < 0.0001$; interaction, $F_{9,104} = 19$, $p < 0.0001$). The estimated ED_{50} value for this effect was 30 mg/g (confidence interval: 11–37).

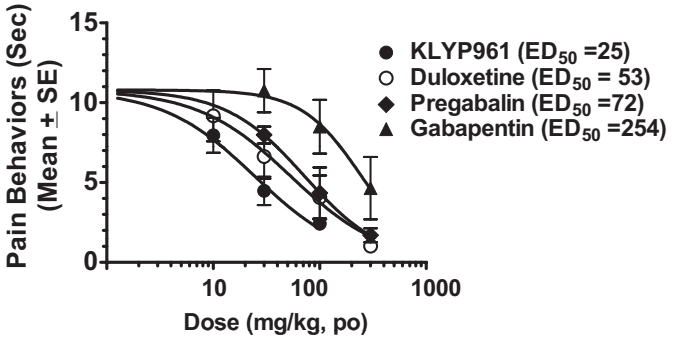

Fig. 4. Orally administered KLYP961, duloxetine, pregabalin, and gabapentin attenuate cold allodynia induced by chronic CCI model. All compounds were administered 60 min before assessment of cold allodynia. Cold allodynia was assessed by monitoring pain behaviors in response to acetone spray. Data represent mean ± S.E. (n = 5–7).

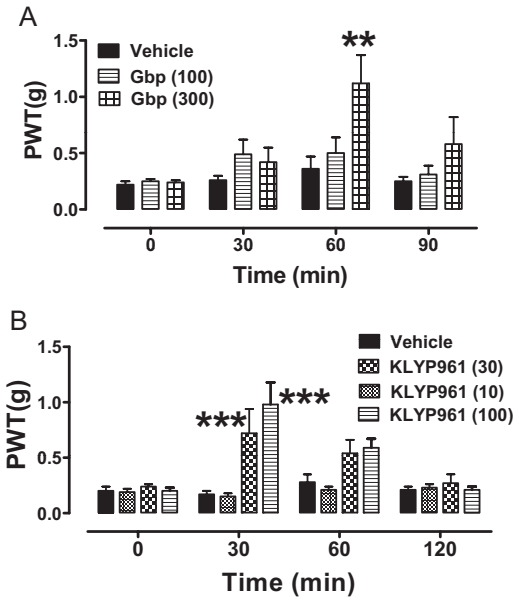

Fig. 5. Orally administered gabapentin (Gbp; A) and KLYP961 (B) attenuate tactile allodynia response after spinal nerve ligation (Chung model) (Kim and Chung, 1992). Tactile allodynia was assessed by monitoring paw withdrawal (PWT) in response to von Frey filaments. Data represent mean ± S.E. (n = 5–6). **, $p < 0.01$ and ***, $p < 0.001$, all relative to vehicle (two-way ANOVA followed by appropriate post hoc test).

In preclinical models, analgesic actions of opiates show tolerance upon repeated dosing. With a view to understanding whether repeated administration of KLYP961 would lead to development of tolerance to its antiallodynic actions, mice that underwent CCI surgery were repeatedly dosed with either KLYP961 (30 mg/kg b.i.d., 3 days), gabapentin (300 mg/kg b.i.d., 3 days), or morphine sulfate (2 mg/kg s.c., b.i.d., 3 days). Animals received one additional dose approximately 16 h after the last dose, i.e., on day 4 for KLYP961 and morphine sulfate groups or day 3 for gabapentin group, and changes in allodynia were measured at preselected time points. Whereas morphine-induced antiallodynic effects tolerated quickly, the effects of KLYP961 or gabapentin were not tolerated. Likewise, the antiallodynic effects of KLYP961 also did not show tolerance in the Chung model (Kim and Chung, 1992) (Supplemental Results S6.3; Supplemental Figs. S3 and S4).

Anti-Inflammatory Activity

Carrageenan Model. Orally administered KLYP961 and celecoxib attenuated carrageenan-induced edema and tactile allodynia in a dose-related manner (Supplemental Fig. S5, A and B) with comparable efficacy and potency. The calculated ED_{50} value for KLYP961 and celecoxib at inhibiting edema were 30 and 45 mg/kg, respectively. The corresponding values for tactile allodynia were 30 mg/kg for both compounds.

Peritoneal Writhing. Intraperitoneal injection of PBQ, an irritant, produces writhing response. Orally administered KLYP961 attenuated writhing response with efficacy and potency comparable with that of celecoxib (Supplemental Fig.

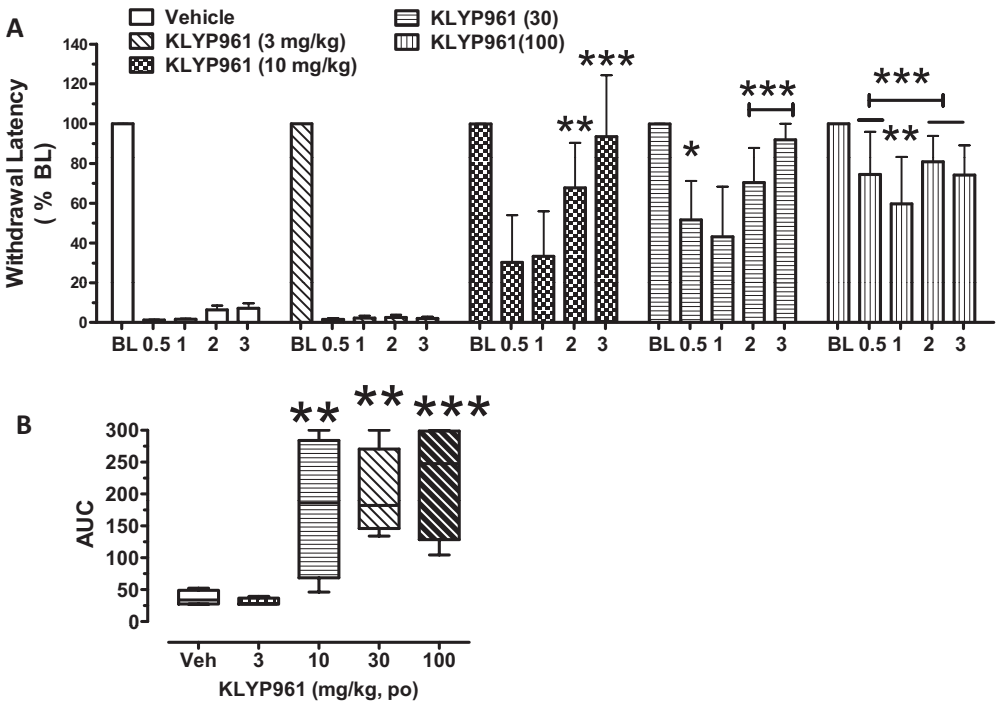

Fig. 6. Topical application of capsaicin-induced thermal hyperalgesia is responsive to KLYP961. Baseline tail withdrawal latencies were measured from 38°C water bath the day before the capsaicin application. After capsaicin application for 15 min (referred to as time 0), tail withdrawal latencies were measured at various times starting at 30 min. Vehicle or KLYP961 were given 60 min before the application of capsaicin patch. Baseline withdrawal latency of each animal was normalized to 100%. AUC data were calculated using the trapezoidal method (GraphPad Prism). Two animals received vehicle and four animals received KLYP961 at each dose level. Animals were given a minimum of 7 days washout before inclusion in the next dose-level testing. Animals were assigned to vehicle or KLYP961 treatments with a crossover between treatments. Withdrawal responses in vehicle-treated animals were pooled. *, $p < 0.05$; **, $p < 0.01$; ***, $p < 0.001$ versus vehicle group [two-way ANOVA for time course (A) or one-way ANOVA (AUC, B)].

S5C). The calculated ED_{50} value for both compounds in this assay was ~100 mg/kg.

Primate Efficacy Studies: Capsaicin-Induced Thermal Allodynia

Chair-trained rhesus primates were used in these experiments. These primates, in the absence of capsaicin treatment, withdrew their tails from a 38°C water bath with a latency of 80 to 120 s. However, after topical application of capsaicin for 15 min, these animals show marked thermal allodynia, reflected in reduced tail withdrawal latencies of <10 s, typically 1 to 5 s. The allodynic responses showed a time course with peak pain responses approximately 1 h after the removal of the capsaicin patch. The animals recovered from the allodynia over 3 to 6 h.

In this model, subcutaneous administration of MK-801 (0.06 mg/kg) led to marked attenuation of established allodynia (Supplemental Results S6.4; Supplemental Fig. S6A). Repeated oral administration of gabapentin at a dose of 60 mg/kg, once a day for 2 days and a third dose on day 3, before application of capsaicin patch, significantly altered the time course of allodynia, whereas a single dose of gabapentin showed a trend for attenuation (Supplemental Fig. S6, B and C).

The dose-related effects of KLYP961 were examined as a pretreatment to capsaicin in the thermal allodynia model. The lowest dose of 3 mg/kg had no effect; as the dose was increased from 10 to 100 mg/kg, there was a dose-related attenuation of allodynia. At 10 and 30 mg/kg, KLYP961 treatment enhanced the recovery from thermal allodynia, and at the highest dose of 100 mg/kg, thermal allodynia was nearly completely abolished (Fig. 6A; treatment, $F_{4,95} = 28$, $p < 0.0001$; time $F_{4,95} = 28.7$, $p < 0.0001$; interaction, $F_{16,95} = 10.9$, $p = 0.02$). The attenuation of thermal allodynia also reflected in significant improvements in AUC (Fig. 6B; $F_{4,19} = 10.3$, $p < 0.0001$).

The effects of KLYP961 on established thermal allodynia were examined at a test dose of 30 mg/kg p.o. Thermal allodynia was assessed 45 min after capsaicin patch removal. Animals were given KLYP961 or vehicle 15 min later, and allodynic responses were measured 1.5, 2, 3, and 4 h after capsaicin patch removal (all times relative to removal of the capsaicin patch). Compared with vehicle treatment, KLYP961 markedly enhanced the rate of recovery of allodynia (Fig. 7A; treatment, $F_{1,64} = 12.4$, $p < 0.0001$; time, $F_{5,64} = 63.4$, $p < 0.0001$; interaction, $F_{5,64} = 10.2$, $p < 0.0001$) and increased AUC ($t = 4.3$, df = 10, $p = 0.0017$; Fig. 7B). These results indicate the ability of KLYP961 to ameliorate established pain states.

Side Effect Profile Studies

Gastrointestinal Transit in Mice. The phenotype of nNOS knockout mice (Mashimo et al., 2000) combined with impairments in gastric motility reported with nonselective inhibitors of all three isoforms of NOS (Orihata and Sarna, 1994) implicate a role for NO derived from NOS isoforms in the regulation of gastric motility. Given that KLYP961 is a dual inhibitor of nNOS and iNOS, the potential impact on gastric motility in a mouse model of charcoal transit was explored. Under subchronic conditions with suprapharmacological doses, KLYP961 did not affect charcoal transit, whereas the experimental positive control, morphine, markedly reduced charcoal transit (Supplemental Results S6.5 and Supplemental Fig. S7).

Motor Coordination in Mice. The effects of administration of single oral doses of KLYP961 on motor coordination were assessed using the rotarod assay with gabapentin as the reference compound. Gabapentin produced dose- and time-dependent impairments in motor coordination. The calculated ED_{50} value for gabapentin, based on its effects at 2 h after dose, was ~140 mg/kg. KLYP961 over the dose range of 100 to 1000 mg/kg did not affect motor performance. Therefore, an ED_{50} value for KLYP961 could not be calculated (Supplemental Results S6.6; Supplemental Fig. S8).

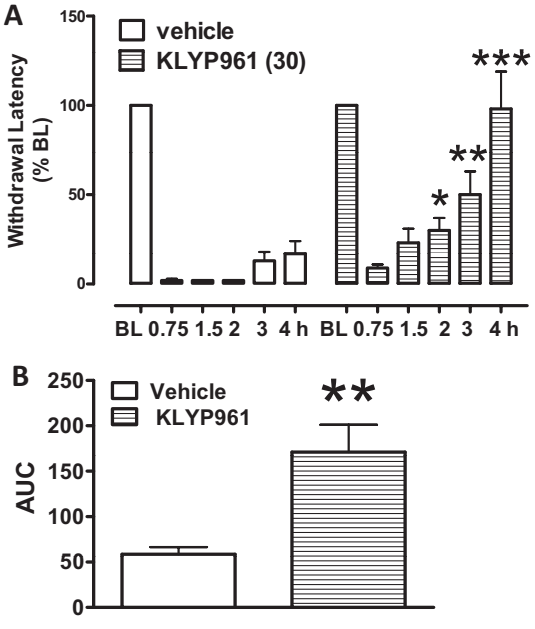

Fig. 7. KLYP961 attenuates capsaicin-induced thermal allodynia when administered in a therapeutic paradigm. Baseline tail withdrawal latencies were measured from 38°C water bath the day before the capsaicin application. After the capsaicin application for 15 min (referred to as time 0), tail withdrawal latencies were measured at various times starting at 45 min (0.75 h). Vehicle or KLYP961 (30 mg/kg) were given at 1 h after capsaicin, and withdrawal latencies were measured at selected times thereafter. Baseline withdrawal latency of each animal was normalized to 100%. AUC data were calculated using the trapezoidal method (GraphPad Prism). Four animals received vehicle and six animals received KLYP961 at 30 mg/kg. Animals were given a minimum of 7 days washout before inclusion in the next dose-level testing. Animals were assigned to vehicle or KLYP961 treatments with a crossover between treatments. Withdrawal responses in vehicle-treated animals were pooled. *, $p < 0.05$; **, $p < 0.01$; ***, $p < 0.001$ versus vehicle group [two-way ANOVA for time course (A) or one way ANOVA (AUC, B)].

Primate Safety Studies: Cardiovascular Studies in Telemetered Cynomolgus Primates. Under the conditions of the experiment, repeated daily dosing with KLYP961 at doses up to 96 mg/kg every day did not adversely affect any systemic cardiovascular hemodynamic or electrocardiographic variables in this model. There were no notable changes in mean arterial pressure (or its associated components, systolic and diastolic arterial pressures), PR interval, or QRS duration (data not shown).

Discussion

Drug discovery efforts to identify selective iNOS inhibitors initially focused on mimetics of arginine. Although many initial substrate mimetics had dose-limiting cardiovascular signals, such as increased blood pressure via inhibition of eNOS, substrate-competitive, time-dependent iNOS inhibitors such as GW274150 with optimum selectivity against eNOS have been identified. The preclinical profile supports a role for NO derived from iNOS in both inflammatory pain and neuropathic pain states (De Alba et al., 2006). In addition to serving as a substrate for NOS isoforms, arginine participates in a physiologically important amino acid metabolic cycle. Substrate competitive inhibitors such as GW274150 can compete with arginine transport mechanisms (Baydoun et al., 2006), but long-term consequences of interference with arginine transport/metabolism are unclear. Inhibition of iNOS dimerization provided another avenue for imparting greater isoform selectivity (Davey et al., 2007). BBS-4, one of the first-generation dimerization inhibitors based on the 2-imidazol-1-ylpyrimidine chemical scaffold, is also a potent inhibitor CYP3A4, thus limiting its use as pharmacological probe. Similar limitations were also noted with chemotypes exemplified by AZ102222C. The pursuit for identification of highly selective pharmacological tools with appropriate drug-like properties culminated in the identification of KLYP961, whose profile is summarized in this article (Bonefous et al., 2009; Payne et al., 2010).

KLYP961 is a dual iNOS/nNOS inhibitor with selectivity against eNOS ranging from approximately 40-fold in mice to 290-fold in primates and 180-fold in humans. Mechanistic studies indicate that KLYP961 affects dimerization of NOS, and the results are consistent with the mechanism of action of KLYP956, a structurally related compound (Symons et al., 2009).

Endotoxin injection in wild-type, but not iNOS knockout, mice produces time-dependent induction of iNOS mainly in the liver, spleen, and kidney accompanied by time-dependent increases in plasma nitrates. KLYP961 attenuated plasma nitrate response with an ED_{50} value of 1 mg/kg. Despite its pharmacokinetic half-life of ~2 h, a dose of 30 mg/kg inhibited nitrate response by 50% for ~12 h, suggesting a pharmacokinetic-pharmacodynamic dichotomy. Changes in plasma nitrates reflect systemic iNOS activity, therefore the time course of changes in plasma nitrates is less likely to mirror the plasma half-life of KLYP961.

KLYP961 attenuated both the acute inflammatory and the secondary nocifensive behavior driven by central sensitization in the formalin model, and the efficacy was both dose- and time-dependent. KLYP961 was more potent at inhibiting phase II behaviors than phase I behaviors. In the latter, KLYP961 was equi-efficacious to, but more potent than, two clinically used agents, gabapentin and pregabalin. A single dose of 30 mg/kg inhibited phase II behavior for up to 4 h, whereas the inhibition of phase I was more transient. With a view to defining the role of NOS inhibition in the formalin response, two structurally related compounds, KLYP322 and KLYP775, were examined that differed in their NOS inhibitory potency profiles. The concordance of efficacy of these two ligands with their NOS inhibitory profiles establishes a causal relationship between NOS inhibition and efficacy. KLYP961 is a dual inhibitor of iNOS and nNOS. Although the precise contribution of inhibition of each isoform to its efficacy is unclear, similar levels of reduction of antinociceptive effects of KLYP961 in both iNOS and nNOS knockout mice relative to wild-type mice, in the formalin model, suggest that dual-inhibition iNOS and nNOS plays a role in its efficacy.

Chronic constriction of the sciatic nerve [the Bennett model (Bennett and Xie, 1988)] leads to a neuropathic pain state evidenced by marked cold allodynia (Walczak and Beaulieu, 2006). In this model. KLYP961 was equi-efficacious to, but more potent than, three clinically used agents, duloxetine, pregabalin, and gabapentin. Consistent with its effects in the Bennett model, KLYP961 also attenuated tactile allodynia in the Chung model (Kim and Chung, 1992). The antiallodynic efficacy of KLYP961 did not show tolerance as was the case with morphine.

A comparison of potency of KLYP961 in various rodent

assays reveals interesting features; the ED_{50} values (mg/kg) in endotoxin, formalin, the Bennett model (Bennett and Xie, 1988), and the Chung model (Kim and Chung, 1992) are 1, 13, 25, and 29 mg/kg, respectively. In addition to the shift in potency, the duration of action of KLYP961(30 mg/kg p.o.) was different in these assays: plasma nitrates (~12 h), formalin (~4 h), and Chung and Bennett (~60–90 min) models. The shift in potency/duration in pain models relative to "plasma nitrate" inhibition assay may reflect the necessity of near-complete inhibition target mechanism for engendering efficacy in pain modality and/or differential sites of action (e.g., NOS inhibition in liver, spleen, and lungs driving the inhibition of nitrate response versus inhibition of NOS in pain pathways along the neuraxis, both central and peripheral). The limited brain penetration of KLYP961 and smaller volume of distribution in mice may also contribute to the dichotomy between plasma nitrate versus efficacy in pain models. Despite its limited central nervous system penetration, KLYP961 has demonstrable activity in neuropathic pain models, suggesting a peripheral component in such models. The clinical utility of topically applied lidocaine attests to the role of peripheral mechanisms in human neuropathic pain states.

KLYP961 demonstrated anti-inflammatory activity in intraplantar carrageenin and intraperitoneal PBQ models with potency and efficacy comparable with that of celecoxib. The precise role and contribution of NO in the above acute inflammation models are unknown, and the shift in potency for KLYP961 in these acute inflammation models relative to its profile in nociception assays summarized above may reflect relative contributions of NO in such models.

Given the greater translational relevance of primate biology to humans, and in light of similarities between primate and human "challenge" pain models (Petersen and Rowbotham, 1999), we sought to examine the profile of KLYP961 in a capsaicin-induced thermal hyperalgesia model in rhesus nonhuman primates, a model that is sensitive to opioid and *N*-methyl-D-aspartate modulation (Butelman et al., 2003). The effects of MK-801 in the present study replicate earlier findings. The model is also sensitive to intervention by gabapentin with greater efficacy seen with repeated administration versus single pretreatment, perhaps reflecting its pharmacokinetics. Qualitatively, gabapentin-treated animals showed a distinct time course of thermal allodynia relative to vehicle-treated animals in that later group, experiencing detectable allodynia only at the 1-h time point with a relative lack of allodynia at all other time points. The time-course profile of gabapentin indicates that it did not abrogate the development of thermal allodynia, but rather delayed the onset and markedly enhanced the recovery. A similar profile was seen for KLYP961; administration to animals with established allodynia resulted in significant enhancement in recovery. These results suggest that KLYP961 is "antihyperalgesic" as opposed to "analgesic," as exemplified by opiate agonist-induced abrogation of allodynia in this model (Butelman et al., 2003).

KLYP961 has minimal off-target activity, desirable drug-like properties such as pharmacokinetic profile, and CYP450 and hERG activities. Acute or subchronic administration of (supra)pharmacological doses of KLYP961 was well tolerated in both mice and primates with acceptable side effect profile in both gastrointestinal motility and cardiovascular function. In addition, KLYP961 has efficacy in a range of pain/inflammation models in both rodents and nonhuman primates. These attributes suggest that KLYP961 has a unique profile relative to known iNOS inhibitors described in the literature (Vallance and Leiper, 2002). The profile of KLYP961 makes it an ideal tool with which to investigate therapeutic utility of iNOS and nNOS inhibition in humans in a variety of disease states where a causal role of NO has been implicated.

Authorship Contributions

Participated in research design: Massari, Rix, Shiau, Noble, Smith, Hassig, Zhang, and Rao.

Conducted experiments: Symons, Nguyen, Anzola, Staszewski, Wang, Yazdani, Dorow, Muhammad, Sablad, Rozenkrants, Bonefous, and Payne.

Performed data analysis: Smith, Hassig, and Zhang.

Wrote or contributed to the writing and review of the manuscript: Shiau, Noble, Smith, Hassig, and Rao.

References

Aley KO, McCarter G, and Levine JD (1998) Nitric oxide signaling in pain and nociceptor sensitization in the rat. *J Neurosci* **18:**7008–7014.

Baydoun AR, Bertran J, Thakur S, Dawson J, Palacín M, and Knowles RG (2006) y+LAT-1 mediates transport of the potent and selective iNOS inhibitor, GW274150, in control J774 macrophages. *Amino Acids* **31:**101–109.

Bennett GJ and Xie YK (1988) A peripheral mononeuropathy in rat that produces disorders of pain sensation like those seen in man. *Pain* **33:**87–107.

Bonnefous C, Payne JE, Roppe J, Zhuang H, Chen X, Symons KT, Nguyen PM, Sablad M, Rozenkrants N, Zhang Y, et al. (2009) Discovery of inducible nitric oxide synthase (iNOS) inhibitor development candidate KLYP961, part 1: Identification of a novel, potent, and selective series of quinolinone iNOS dimerization inhibitors that are orally active in rodent pain models. *J Med Chem* **52:**3047–3062.

Butelman ER, Ball JW, Harris TJ, and Kreek MJ (2003) Topical capsaicin-induced allodynia in unanesthetized primates: pharmacological modulation. *J Pharmacol Exp Ther* **306:**1106–1114.

Davey DD, Adler M, Arnaiz D, Eagen K, Erickson S, Guilford W, Kenrick M, Morrissey MM, Ohlmeyer M, Pan G, et al. (2007) Design, synthesis, and activity of 2-imidazol-1-ylpyrimidine derived inducible nitric oxide synthase dimerization inhibitors. *J Med Chem* **50:**1146–1157.

De Alba J, Clayton NM, Collins SD, Colthup P, Chessell I, and Knowles RG (2006) GW274150, a novel and highly selective inhibitor of the inducible isoform of nitric oxide synthase (iNOS), shows analgesic effects in rat models of inflammatory and neuropathic pain. *Pain* **120:**170–181.

Dunham NW and Miya TS (1957) A note on a simple apparatus for detecting neurological deficit in rats and mice. *J Am Pharm Assoc* **46:**208–209.

Goettl VM and Larson AA (1996) Nitric oxide mediates long-term hyperalgesic and antinociceptive effects of the N-terminus of substance P in the formalin assay in mice. *Pain* **67:**435–441.

Haley JE, Dickenson AH, and Schachter M (1992) Electrophysiological evidence for a role of nitric oxide in prolonged chemical nociception in the rat. *Neuropharmacology* **31:**251–258.

Holthusen H and Arndt JO (1994) Nitric oxide evokes pain in humans on intracutaneous injection. *Neurosci Lett* **165:**71–74.

Kawabata A, Manabe S, Manabe Y, and Takagi H (1994) Effect of topical administration of L-arginine on formalin-induced nociception in the mouse: a dual role of peripherally formed NO in pain modulation. *Br J Pharmacol* **112:**547–550.

Kim SH and Chung JM (1992) An experimental model for peripheral neuropathy produced by segmental spinal nerve ligation in the rat. *Pain* **50:**355–363.

Kolodziejski PJ, Koo JS, and Eissa NT (2004) Regulation of inducible nitric oxide synthase by rapid cellular turnover and co-translational down-regulation by dimerization inhibitors. *Proc Natl Acad Sci USA* **101:**18141–18146.

LaBuda CJ, Koblish M, Tuthill P, Dolle RE, and Little PJ (2006) Antinociceptive activity of the selective iNOS inhibitor AR-C102222 in rodent models of inflammatory, neuropathic and post-operative pain. *Eur J Pain* **10:**505–512.

Levy D and Zochodne DW (1998) Local nitric oxide synthase activity in a model of neuropathic pain. *Eur J Neurosci* **10:**1846–1855.

Levy D, Höke A, and Zochodne DW (1999) Local expression of inducible nitric oxide synthase in an animal model of neuropathic pain. *Neurosci Lett* **260:**207–209.

Lin Q, Palecek J, Palecková V, Peng YB, Wu J, Cui M, and Willis WD (1999) Nitric oxide mediates the central sensitization of primate spinothalamic tract neurons. *J Neurophysiol* **81:**1075–1085.

Malmberg AB and Yaksh TL (1993) Spinal nitric oxide synthesis inhibition blocks NMDA-induced thermal hyperalgesia and produces antinociception in the formalin test in rats. *Pain* **54:**291–300.

Mashimo H, Kjellin A, and Goyal RK (2000) Gastric stasis in neuronal nitric oxide synthase deficient mice. *Gastroenterology* **119:**766–773.

Meller ST and Gebhart GF (1993) Nitric oxide (NO) and nociceptive processing in the spinal cord. *Pain* **52:**127–136.

Orihata M and Sarna SK (1994) Inhibition of nitric oxide synthase delays gastric emptying of solid meals. *J Pharmacol Exp Ther* **271:**660–670.

Payne JE, Bonnefous C, Symons KT, Nguyen PM, Sablad M, Rozenkrants N, Zhang Y, Wang L, Yazdani N, Shiau AK, et al. (2010) Discovery of dual inducible/neuronal nitric oxide synthase (iNOS/nNOS) inhibitor development candidate KD7332 (part 2): Identification of a novel, potent, and selective series of benzimid-

azole-quinolinone iNOS/nNOS dimerization inhibitors that are orally active in pain models. *J Med Chem* **53:**7739–7755.
Petersen KL and Rowbotham MC (1999) A new human experimental pain model: the heat/capsaicin sensitization model. *Neuroreport* **10:**1511–1516.
Symons KT, Massari ME, Nguyen PM, Lee TT, Roppe J, Bonnefous C, Payne JE, Smith ND, Noble SA, Sablad M, et al. (2009) KLYP956 is a non-imidazole-based orally active inhibitor of nitric oxide synthase dimerization. *Mol Pharmacol* **76:** 153–162.
Tang Q, Svensson CI, Fitzsimmons B, Webb M, Yaksh TL, and Hua XY (2007) Inhibition of spinal constitutive NOS-2 by 1400W attenuates tissue injury and inflammation-induced hyperalgesia and spinal p38 activation (2007). *Eur J Neurosci* **25:**2964–2972.
Tao F, Tao YX, Mao P, Zhao C, Li D, Liaw WJ, Raja SN, and Johns RA (2003) Intact carrageenan-induced thermal hyperalgesia in mice lacking inducible nitric oxide synthase. *Neuroscience* **120:**847–854.
Vallance P and Leiper J (2002) Blocking NO synthesis: how, where and why? *Nat Rev Drug Discov* **1:**939–950.
Walczak JS and Beaulieu P (2006) Comparison of three models of neuropathic pain in mice using a new method to assess cold allodynia: the double plate technique. *Neurosci Lett* **399:**240–244.
Wu J, Fang L, Lin Q, and Willis WD (2001) Nitric oxide synthase in spinal cord central sensitization following intradermal injection of capsaicin. *Pain* **94:**47–58.
Yamamoto T, Shimoyama N, and Mizuguchi T (1993) Nitric oxide synthase inhibitor blocks spinal sensitization induced by formalin injection into the rat paw. *Anesth Analg* **77:**886–890.

Address correspondence to: Dr. Tadimeti S. Rao, Johnson and Johnson, 3210 Merryfield Row, San Diego, CA 92121. E-mail: trao1@its.jnj.com